

GTOC X: SETTLERS OF THE GALAXY PROBLEM DESCRIPTION AND SUMMARY OF THE RESULTS

**Anastassios E. Petropoulos^{*}, Eric D. Gustafson[†],
Gregory J. Whiffen[‡], and Brian D. Anderson[§]**

The Global Trajectory Optimisation Competition was inaugurated in 2005 by Dario Izzo of the Advanced Concepts Team, European Space Agency, as a means of fostering innovation in trajectory design and cross-fertilisation with other fields. GTOC2 through GTOC9 were organized by the winning teams of the preceding GTOC editions. Keeping this tradition, the Outer Planet Mission Analysis Group and Mission Design and Navigation Section of the Jet Propulsion Laboratory organized the tenth edition of the competition, GTOC X. The futuristic problem posed may loosely be described as a “Settlers of the Galaxy” challenge, wherein trajectories must be designed for humanity to settle throughout the galaxy. After the release of the precise problem statement, the 73 registered teams had four weeks to work on the problem. Solutions were submitted to the competition website for automated verification and scoring on a leaderboard. A total of 42 teams returned solutions. In this paper we describe the GTOC X problem, and give an overview of the solutions and their verification and ranking. Six teams presented their work at a special GTOC X session of this Conference, including the winning team led jointly by the National University of Defense Technology and the Xi’an Satellite Control Center, both of China.

INTRODUCTION

The Global Trajectory Optimisation Competition was inaugurated in 2005 by Dario Izzo of the Advanced Concepts Team, European Space Agency, as a means of fostering innovation in trajectory design and cross-fertilisation with other fields.¹ GTOC2 through GTOC9 were organized by the winning teams of the preceding GTOC editions. Keeping this tradition, the Outer Planet Mission Analysis Group and Mission Design and Navigation Section of the Jet Propulsion Laboratory organized the tenth edition of the competition, GTOC X.

The criteria for selecting, or perhaps one should say, designing, the GTOC X problem are similar to those used in the previous competitions: Global optimization over a large design space with many local optima; unusual objective function, or constraints — no canned methods or existing software can likely fully solve the problem; problem is easy enough to tackle in a 3-4 week timeframe

^{*}Engineer, Mission Design and Navigation Section, Jet Propulsion Laboratory, California Institute of Technology, Pasadena, CA 91109.

[†]Engineer, Mission Design and Navigation Section, Jet Propulsion Laboratory, California Institute of Technology, Pasadena, CA 91109.

[‡]Engineer, Mission Design and Navigation Section, Jet Propulsion Laboratory, California Institute of Technology, Pasadena, CA 91109.

[§]Engineer, Mission Design and Navigation Section, Jet Propulsion Laboratory, California Institute of Technology, Pasadena, CA 91109.

©2019. California Institute of Technology. Government sponsorship acknowledged.

for experienced mission designers or mathematicians, including exploration of new algorithms; problem solutions can be easily verified. The problem chosen this year added the dimension of unfamiliar trajectory dynamics, and, so to speak, a much larger playing field.

In this paper, we describe first the GTOC X problem as posed to the participating teams. The subsequent sections will describe the development of the problem, the competition logistics, and an overview of the solutions that were submitted. The present paper, together with papers from six of the top teams, comprised a special session on GTOC X at the conference. The winning solution was submitted by a joint team from the National University of Defense Technology in Beijing, China, and the Xi'an Satellite Control Center, in Xi'an, China.

THE SCENARIO

In about ten thousand years from the present, humanity will reset its counting of years to zero. Year Zero will be the year when humanity decides the time is ripe for the human race to boldly venture into the galaxy and settle other star systems. One hundred thousand star systems in the galaxy have been identified as being suitable for settlement. Even in this Year Zero, although technologies and knowledge have dramatically progressed, we are still subject to the tyranny of inertia and remain far from the near-instantaneous space travel depicted fancifully in science fiction. However, enormous strides have been made in the ability to live in space, so much so that self-reliant settler vessels can travel through space for hundreds of thousands of generations, making it possible for humans to reach and settle other star systems. The task in GTOC X is to settle as many of the one hundred thousand star systems as possible, in as uniform a spatial distribution as possible, while using as little propulsive velocity change as possible. The settlement of the galaxy starts by fanning out from our home star, Sol. Once another star is settled, further settlements can fan out from that star. Solutions that are submitted earlier rather than later in the submission period will be rewarded a bonus stemming from the fact that humanity's resources are dwindling and the sooner we decide on a settlement plan for the galaxy, the better.

THE PROBLEM

The stars that are available for settlement are defined in a database file, `stars.txt`. They are all in circular orbits around the galactic center; their ephemerides are described in the "Equations and Ephemerides" section. The initial settlers from Sol depart in up to three **Mother Ships** and up to two **Fast Ships**. All departures from Sol must occur no later than 10 Myr (10 million years) past Year Zero. Mother Ships each carry up to 10 **Settlement Pods**; a Settlement Pod is released at the instant when the Mother Ship flies by a star (*i.e.*, matches the position of the star). The Settlement Pod's velocity is equal to the Mother Ship's velocity at the instant of release, whereupon the Settlement Pod immediately performs a maneuver to match the velocity of the star, thereby settling that star. The Mother Ship's velocity is unaffected by the flyby (*i.e.*, there is no gravity assist, the star is a massless, moving point in space). The Fast Ships can each rendezvous with a single star (*i.e.*, match its position and velocity), which is then considered settled. Up to three **Settler Ships** can depart from each settled star, as long as at least 2 Myr have elapsed since the star became settled. Each Settler Ship can rendezvous with a single star, which is then considered settled. Stars can only be settled once.

The motion of the ships is subject to the central-force law described in the "Equations and Ephemerides" section. The ships and pods execute impulsive maneuvers to control their motion, as described in the "Propulsive Maneuvers" section. Settlements can be made up to 90 Myr past

Year Zero. The task of the competition is to design the trajectories of these ships (*i.e.*, a settlement tree) to maximize the merit function described in section “Merit Function”.

Equations and Ephemerides

A central-force law governs the motion of both the stars and the ships. The ephemerides of the stars are available analytically because they are assumed to follow circular orbits. The central-force law assumed for the competition approximately models the circular motion observed for actual stars in our Milky Way. Specifically, the circular orbit speed, v_c , for a body at radius r from the galactic center, and the acceleration, f , directed towards the galactic center are

$$v_c(r) = \frac{1}{k_8 r^8 + k_7 r^7 + k_6 r^6 + k_5 r^5 + k_4 r^4 + k_3 r^3 + k_2 r^2 + k_1 r + k_0} \quad (1)$$

$$f(r) = \frac{v_c^2}{r} \quad (2)$$

where the k_i ($i = 0, \dots, 8$) are constants defined in the “Constants and Conversions” section. The Cartesian position coordinates of any body (x, y, z) obey the differential equations with respect to time, t :

$$\frac{d^2 x}{dt^2} = -\frac{x}{r} f(r) \quad (3)$$

$$\frac{d^2 y}{dt^2} = -\frac{y}{r} f(r) \quad (4)$$

$$\frac{d^2 z}{dt^2} = -\frac{z}{r} f(r) \quad (5)$$

where $r = \sqrt{x^2 + y^2 + z^2}$.

The motion of the stars also obeys these differential equations, but, due to their orbits being circular, the motion can be expressed analytically and so the following equations should be used to determine position and velocity for the stars as a function of time past Year Zero, t :

$$n \equiv v_c(R)/R \quad (6)$$

$$x = R[\cos(nt + \phi) \cos \Omega - \sin(nt + \phi) \cos i \sin \Omega] \quad (7)$$

$$y = R[\cos(nt + \phi) \sin \Omega + \sin(nt + \phi) \cos i \cos \Omega] \quad (8)$$

$$z = R[\sin(nt + \phi) \sin i] \quad (9)$$

$$v_x = v_c(R)[- \sin(nt + \phi) \cos \Omega - \cos(nt + \phi) \cos i \sin \Omega] \quad (10)$$

$$v_y = v_c(R)[- \sin(nt + \phi) \sin \Omega + \cos(nt + \phi) \cos i \cos \Omega] \quad (11)$$

$$v_z = v_c(R)[\cos(nt + \phi) \sin i] \quad (12)$$

where the values of R, i, Ω, ϕ for each star are specified in a provided ASCII data file, `stars.txt`, which has one header line followed by one line for each star, including Sol. Stars are assigned integer identifiers (IDs) in the file, starting with 0 for Sol and progressing to 100,000. The final column in the file, given for convenience, is the final polar angle of the star which is a derived quantity: $\theta_f = \text{atan2}(y(t_f), x(t_f))$, $t_f = 90$ Myr. It should be noted that we are following common galactic conventions: We take the $+z$ direction as the Galactic North direction and so the stars are orbiting in a retrograde direction around this axis (clockwise when looking down on the galaxy from Galactic North); that is why, for the above equations, the inclinations, i , listed in the file approach 180 degrees.

Propulsive Maneuvers

Propulsive maneuvers are impulsive, meaning that the velocity of the ship (or pod) changes instantaneously when the impulse is applied. The magnitude of the change in velocity due to an impulse is denoted ' ΔV '. The limits on the magnitude and number of ΔV s are listed in Table 1.

In addition, there is a timing constraint on the maneuvers. For a given ship, consecutive maneuvers must be spaced at least 1 Myr apart in time. A Settlement Pod's rendezvous impulse must also be separated by at least 1 Myr from any impulses performed by the Mother Ship or by any other Settlement Pod from the same Mother Ship. Figure 1 provides a schematic view of a settlement tree starting from Sol.

Table 1. Propulsive Maneuver Limits

Type of vessel	Available Number of Impulses	Maximum single impulse	Maximum Total ΔV
Mother Ship	3	200 km/s	500 km/s
Settlement Pod	1	300 km/s	300 km/s
Fast Ship	2	1500 km/s	1500 km/s
Settler Ship	5	175 km/s	400 km/s

Other Constraints and Tolerances

Ships must not venture closer than 2 kpc to the galactic center, nor further than 32 kpc:

$$2 \text{ kpc} \leq r(t) \leq 32 \text{ kpc}, \quad \forall t \quad (13)$$

Upon submission via the competition website, solutions will be checked against our independent propagations generated from the submitted data. Solutions will have to meet the following tolerances to be considered valid:

- Violation of limits on magnitudes of individual ΔV s and Total ΔV per vessel: 0.01 km/s.
- Error in magnitude of arrival impulse: 0.01 km/s.
- Violation of maneuver timing limits and 90 Myr time limit: 1 yr.
- Error in position of vessel with respect to star at rendezvous epoch: 10^{-4} kpc.
- Violation of range limits (Eq. 13): 0.01 kpc.

Merit Function

We define first a number of auxiliary equations. Let N be the number of settled stars. Sol does not count as a settled star. First we define the function f of a variable x and parameters μ, s :

$$f(x; \mu, s) = \begin{cases} 0, & |x - \mu| \geq s \\ \frac{1}{s} - \frac{|x - \mu|}{s^2}, & \text{otherwise.} \end{cases} \quad (14)$$

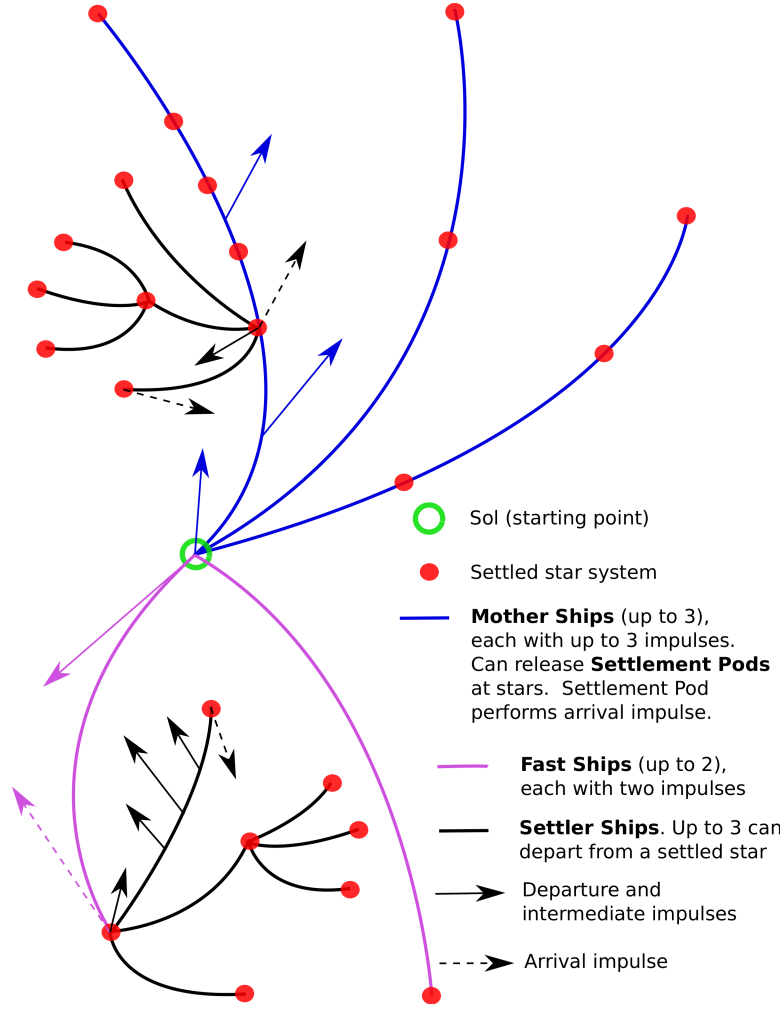


Figure 1. Schematic of a settlement tree fanning out from Sol. Only some impulses are shown: Three for one of the Mother Ships, two for one of the Fast Ships, one for a Settlement Pod, two for one Settler Ship, and five for another Settler Ship.

For the radial and angular coordinates, we then define:

$$f_r(r) = \frac{1}{N} \sum_{i=1}^N f(r; r_i, s_r) \quad (15)$$

$$f_\theta(\theta) = \frac{1}{N} \sum_{i=1}^N f(\theta; \theta_i, s_\theta) \quad (16)$$

where $s_r = 1.0$ kpc, $s_\theta = 2\pi/32$ rad, r_i is the orbital radius of the i^{th} settled star, and θ_i is the final polar angle, θ_f , of the i^{th} settled star (as given in the `stars.txt` file).

Additionally, with $R_{\min} = 2$ kpc and $R_{\max} = 32$ kpc, we define the goal functions and param-

ters:

$$g_r(r) = \alpha(r) \frac{2r}{R_{\max}^2 - R_{\min}^2} \quad (17)$$

$$g_\theta(\theta) = \beta(\theta) \frac{1}{2\pi} \quad (18)$$

$$R_k = k + 2 \text{ kpc}, \quad 0 \leq k \leq 30 \quad (19)$$

$$\Theta_k = -\pi + 2\pi \frac{k}{32} \text{ rad}, \quad 0 \leq k \leq 32 \quad (20)$$

where the scaling functions α and β are

$$\alpha(r) = \begin{cases} 0.5833, & r = 2 \text{ kpc} \\ 0.4948, & r = 32 \text{ kpc} \\ 1, & \text{otherwise.} \end{cases} \quad (21)$$

$$\beta(\theta) = \begin{cases} 0.5, & \theta = -\pi \text{ rad} \\ 0.5, & \theta = \pi \text{ rad} \\ 1, & \text{otherwise.} \end{cases} \quad (22)$$

The following error functions can then be defined:

$$E_r = \sum_{k=0}^{30} \left(\frac{f_r(R_k)}{g_r(R_k)} - 1 \right)^2 \quad (23)$$

$$E_\theta = \sum_{k=0}^{32} \left(\frac{f_\theta(\Theta_k)}{g_\theta(\Theta_k)} - 1 \right)^2 \quad (24)$$

A bonus factor for submitting a solution early is also defined as:

$$B = 1 + \left(\frac{t_{\text{end}} - t_{\text{submission}}}{t_{\text{end}} - t_{\text{start}}} \right)^4, \quad (25)$$

where t_{start} and t_{end} are the start and end epochs of the GTOC X solution submission timeframe, and $t_{\text{submission}}$ is the epoch at which the solution file is submitted and received at the GTOC X website. The start and end epochs were May 21, 2019, 8p.m. UTC, and June 12, 2019, 8 p.m. UTC.

Finally, the merit function, J , to be maximized is the following:

$$J = B \left(\frac{N}{1 + 10^{-4} \cdot N(E_r + E_\theta)} \right) \left(\frac{\Delta V_{\max}}{\Delta V_{\text{used}}} \right), \quad (26)$$

where ΔV_{used} is the total ΔV used in the settlement tree (the sum of all impulses performed by each ship and pod) and ΔV_{\max} is maximum ΔV permitted, obtained by summing each vessel's Maximum Total ΔV shown in Table 1. Should there be a tie to five significant figures in J , the tree with larger N will win. Should there still be a tie, the solution with the smaller ΔV_{used} will win.

Constants and Conversions

The values for the necessary constants and unit conversions are shown in Table 2. Two of the less customary units used, at least in the field of spacecraft trajectory design, are Myr (million years) and kpc (kiloparsecs).

Table 2. Constants and unit conversions

Constant	Value	Units
k_8	-1.94316e-12	(km/s) ⁻¹ /kpc ⁸
k_7	3.7516e-10	(km/s) ⁻¹ /kpc ⁷
k_6	-2.70559e-08	(km/s) ⁻¹ /kpc ⁶
k_5	9.70521e-07	(km/s) ⁻¹ /kpc ⁵
k_4	-1.88428e-05	(km/s) ⁻¹ /kpc ⁴
k_3	0.000198502	(km/s) ⁻¹ /kpc ³
k_2	-0.0010625	(km/s) ⁻¹ /kpc ²
k_1	0.0023821	(km/s) ⁻¹ /kpc
k_0	0.00287729	(km/s) ⁻¹
1 kpc	30856775814671900	km
1 Myr	10 ⁶	yr
1 yr	31557600	s

PROBLEM DEVELOPMENT

While searching for unfamiliar trajectory dynamics on which to base GTOC X, we simultaneously sought a problem that would particularly captivate the imagination, especially since this is the tenth GTOC, the first double-digit GTOC in our customary base-10 counting. Many aspects of the chosen problem are of course contrived, however, one aspect in particular is based on well-studied physics, namely the galactic rotation curve. Galactic dynamics have many intricacies,² but one fundamental feature of spiral galaxies is that the rotation curve is more or less flat, *i.e.*, the bulk of stars in the galaxy move at roughly the same speed around the galactic center (to within ten or twenty percent). From the rotation curve, in turn, can be inferred a central-force law, to which any intra-galactic spacecraft would also be subject. The next sections will describe how a rotation curve was selected for the Milky Way, how an initial set of stars was assembled, and how the merit function and constraints for the problem were developed.

ROTATION CURVE OF THE MILKY WAY

Even with recent unprecedented advances in our knowledge of the structure of our own galaxy,³⁻⁷ there is still considerable uncertainty in the rotation curve of the Milky Way. The rotation curve defined by Eq. 1 was developed by fitting the circular velocity data presented in Bhattacharjee *et al.*,⁵ specifically Table 2 therein which includes uncertainty estimates on the velocity. An inverse polynomial fit was chosen for its simplicity and ability to fit the data using a relatively low order. The fit was restricted to cover the range from 2-32 kpc, roughly double the radius of the visible disk of the Milky Way, and excluding the galactic center. As shown in Fig. 2, a number of points are excluded from the fit, and three artificial points are added to help shape the fit more easily.

ASSEMBLING THE SET OF SETTLEABLE STARS

The choice to use an artificial galaxy

When choosing the galactic playing field for GTOC X, we would have ideally used the actual positions of the stars in our own Milky Way galaxy as obtained from the Gaia mission.^{3,6,7} However, the star catalogs available have large uncertainties for the radial distance from Earth for many of the

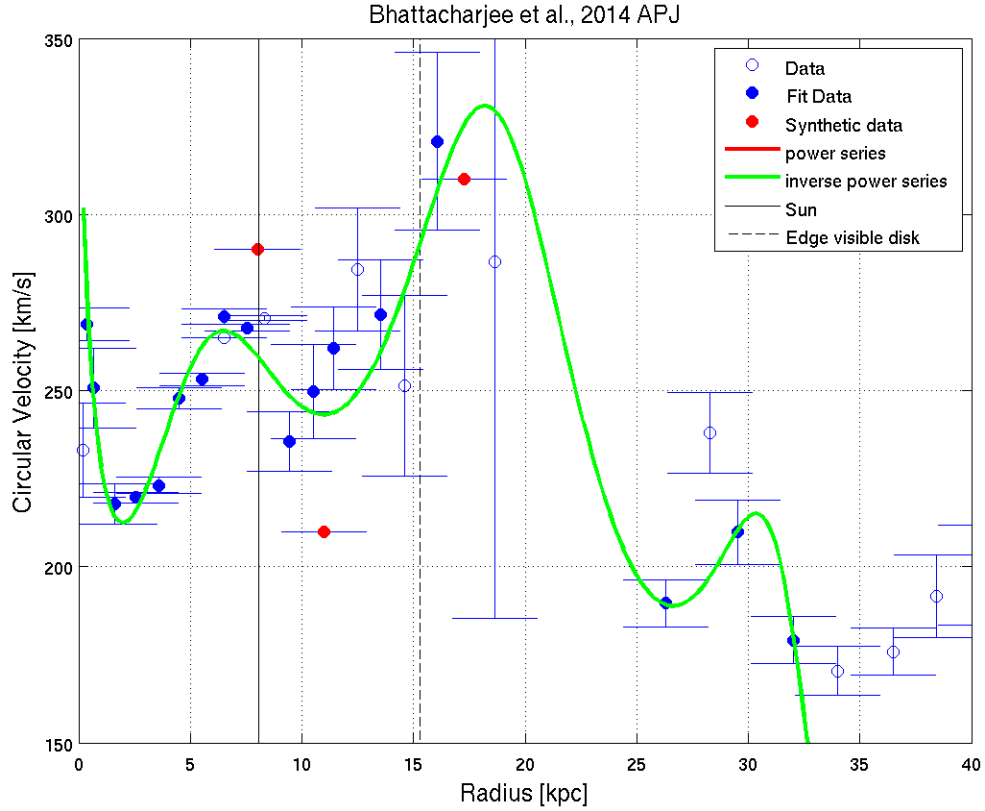


Figure 2. Fit of the rotation curve for the Milky Way.

stars.⁸ This is an inherent limitation of the parallax method of measuring star distance as the Earth orbits the Sun. The maximum baseline of approximately 1 AU sets a hard limit on one parameter that can improve the radial distance measurement resolution. The remaining parameter for improving the measurement is to increase the resolution of angular measurements, which is a difficult engineering problem. Since this limits our capabilities of reproducing a 3D representation of the stars in our galaxy, we chose to use an artificial galaxy for the competition. The final set of stars is the result of combining an N-body numerical simulation with statistical sampling. The following sections will cover the details.

Initial, realistic galaxy: N-body simulation

We chose to use a galaxy with 1×10^5 stars for the competition. However, we opted to use 5×10^5 particles for the numerical simulations, as we found this produced more realistic structures when propagated. The initial conditions for the simulations were relatively uniform, but the evolution of the stars within the dynamical model of gravity produces more interesting distributions similar to those of observed galaxies. Once a fitting spiral-arm galaxy distribution was achieved, the states of the stars were used for the next step in producing the GTOC X initial galaxy state. The initial positions of the stars were randomly sampled in a cylindrical volume with an elliptical cross-section. The height of the cylinder was fixed to 12 kly and its major axis was fixed to 120 kly. We chose

this size since an initial particle cluster of this size evolved into a galaxy roughly the same size as the Milky Way. When fitting the rotation curve of the Milky Way, as described above, we used 32 kpc (≈ 104 kly) to represent the edge of the Milky Way, and a recent study by Watkins *et al.* to estimate its total mass used 39.5 kpc as the outer limit.⁹ The flattening of the sampling volume cross section was varied to generate different data sets, and the value selected for the final data set was $f = 0.3$. We chose this value since it resulted in a spiral galaxy with two arms and a central bulge at the core. Additionally, the initial transverse velocity of each particle was chosen in order to achieve a fixed angular velocity, parallel to the xy-plane and perpendicular to the radius vector. Each simulation had a fixed value of the initial angular velocity, and we varied it in the following range for the various simulations:

$$V_{t,i} = \omega |\vec{r}_i|, \quad 4.0 \times 10^{-17} \text{ rad/s} \leq \omega \leq 7.0 \times 10^{-17} \text{ rad/s} \quad (27)$$

A clockwise rotation of the galaxy was desired, and thus the direction of the tangential component was chosen to be clockwise as well. The initial velocity components in the radial and out-of-plane directions were set to zero. We chose this range of angular velocities since it was a set that in general prevented the galaxy from expanding too much or indefinitely as it evolved. The final data set used $\omega = 6.7 \times 10^{-17} \text{ rad/s}$.

An all-pairs propagation for an N-body problem using Newton's universal law of gravitation has the familiar computational complexity of $O(n^2)$. Since we were computing galaxies of order 10^5 stars, this was counter-productive, so we opted to use an approximate, but more efficient algorithm. For this purpose, we chose the Barnes-Hut N-body algorithm, see Barnes and Hut.¹⁰ When computing the force on a particle due to the $(n - 1)$ other particles, this algorithm approximates a distant cluster of attracting bodies as a point mass at the cluster's center of mass with the combined mass of the cluster. The more distant the cluster is, the larger the volume in which all bodies are approximated as a single point mass becomes. The forces due to nearby particles are explicitly computed without approximation. This algorithm reduces an N-body simulation to complexity $O(n \log(n))$. In particular, we used the algorithm as implemented by Mateus Zitelli.¹¹ The Barnes-Hut algorithm solidifies the force law, and for the propagation we used a fixed step Euler method. The time step used for the propagation was $dt = 5 \times 10^{13} \text{ s} \approx 1.584 \text{ Myr}$. We used a combination of two simulated data sets as inputs to the refinement step in the next section. These two data sets are in fact two instantaneous galaxy states taken from the same simulation at $t = 400dt \approx 633.8 \text{ Myr}$ and $t = 1200dt \approx 1901.3 \text{ Myr}$. These sets were chosen such that four spiral arms would be present in the galaxy.

Creating a better playing field: hybrid of simulations and random samples

One of the intentions of the problem was to encourage teams to settle the galaxy in a somewhat distributed manner, achieving something like a settlement density that is constant per unit area. This sort of distribution has settlement density proportional to r^2 , which is dramatically at odds with real galactic star densities. So, to ensure the hope of distributed settlements didn't conflict too strongly with the actual distribution of available stars, we used a hybrid approach which combined stars from realistic N-body simulations with stars simply drawn from the desired distribution. The simulated stars were chosen from two runs containing two prominent spiral arms each. The stars from these simulations were combined to provide a data set with four spiral arms. From the raw sets of star simulations, several modifications were made. First, the stars with the largest 1% of radius were treated as outliers and removed. Next, the radii of all stars was scaled to be at a maximum of 32

kpc. After that scaling, all stars with radius less than 2 kpc were removed. Finally, all stars with inclination less than 100° were removed.

For the randomly selected stars, radius values were chosen by

$$r = \sqrt{2^2 + (32^2 - 2^2)z}, \quad (28)$$

where z is a uniform random variable on the range $[0, 1]$. This yields radius values with density proportional to r^2 as required for an equal-area distribution. The inclination was chosen randomly, but limited such that the maximum out-of-plane position component would be less than 5 kpc. The other angular elements were chosen uniformly randomly in $[0, 2\pi]$.

In the end, the published set of stars consisted of 80,000 stars from the N-body simulations and 20,000 randomly selected stars. The star positions are depicted in Figs. 3 and 4.

DEVELOPING THE MERIT FUNCTION

The development of the merit function started with a brainstorming session where many possible approaches were discussed. An initial topic was even just which aspects of the settlement problem should be scored, such as wall-clock time, propellant usage, uniformity of settlement distribution, *etc.*

Most of the focus was on how to efficiently score the uniformity of settlement. Initial thinking was that a covariance-based approach would be the most effective. After all, it is easy to compute and has the feature that maximizing the covariance tends to spread out settlements. However, maximization of covariances tends to push solution to the boundaries of the problems, neglecting the interior space. Approaches such as discrete binning were considered, but suffer from numerical tolerance issues where slight perturbations can cause a merit function to change disproportionately to the solution.

Eventually, we settled on an approach based on probability distribution functions (PDFs). In short, the radial and angular components of a settlement's position were scored on how well they matched a distribution that is evenly spread over area. Given the minimum and maximum allowable radii for the problem (R_{\min} and R_{\max}), this gives a radial PDF of

$$p_r(r) = \frac{2r}{R_{\max}^2 - R_{\min}^2}. \quad (29)$$

Note that the area of $g_r(r)$ between R_{\min} and R_{\max} is one, as required by a valid PDF. The angular component is a simpler uniform distribution:

$$p_\theta(\theta) = \frac{1}{2\pi}. \quad (30)$$

Once the goal PDFs are defined, the next consideration is how to construct a PDF from the settlements, given that they are discrete values. The idea was to build the PDF from a combination of basis functions. Each basis function is its own PDF, with the peak value at the settlement value, and tapering to zero for nearby points. The triangular distribution was chosen for its simplicity and finite support. This avoids any drawbacks of discrete binning. The main drawback of this approach is that for points that adhere to the desired distribution, the basis functions don't combine exactly to reproduce the goal pdf at the boundary points. This is the reason for the α and β coefficients

in the problem statement $g_r()$ and $g_\theta()$ functions. For the radial functions, defining $F(x)$ as the Cumulative Distribution Function (CDF) of the basis function's PDF, the value of the PDF in the limit of many infinitesimally spaced settlements following the goal distribution, we have the value of the combined basis function as any point x :

$$f_x(x) = \frac{2}{R_{\max}^2 - R_{\min}^2} x [F(R_{\max} - x) - F(R_{\min} - x)] + \quad (31)$$

$$\frac{2}{R_{\max}^2 - R_{\min}^2} \left\{ [z \cdot F(z)]_{R_{\min}-x}^{R_{\max}-x} - \int_{R_{\min}-x}^{R_{\max}-x} F(z) dz \right\}. \quad (32)$$

For the angular component, things simplify because the goal distribution has zero slope:

$$f_x(x) = \frac{1}{2\pi} [F(2\pi - x) - F(-x)] \quad (33)$$

These seemingly complicated formulas only really matter at the endpoints. At all interior points, the PDF obtained as the combination of basis functions is identical to the goal PDF. The values of α and β given in the problem description are these functions evaluated at the endpoint values. Again, the point of this correction is to account for boundary effects introduced by the use of basis functions.

The number of stars settled, N , should also logically play a role in the merit function. Larger N should be rewarded, as long as it does not come at the expense of poorer spatial distributions. To this end, the ratio shown in the merit function (Eq. 26) is used, with a weighting factor of 10^{-4} to relate N to the spatial distribution (error) terms, so that J is not too sensitive either to N or to $(E_r + E_\theta)$.

Of course, ΔV consumption is a traditional mission design metric, and so it is also included in the merit function, but as a somewhat unusual ratio of ΔV available to ΔV used. This ratio, has the potential to be a very strong lever in advancing the merit function.

The final component of the merit function is the time bonus factor, B . The value of B drops from two to one in proportion to the fourth power of the time elapsed since the opening of the submission period. The purpose of the time bonus was to encourage teams to submit solutions earlier so that the leaderboard would contribute to an active and robust competition.

RESULTS

A total of 42 teams submitted solutions throughout the competition timeframe via the competition website.¹² Solutions were automatically checked on the web server. Verified solutions were ranked on a public, real-time leaderboard if they improved upon a team's earlier solution. The final results of the top 25 teams are presented in Table 3. The full leaderboard and other details of the competition may be found on the competition website.

Early on, a number of teams exploited the ΔV ratio and the time bonus, quickly finding one or a handful of very-low- ΔV transfers, especially with Fast Ships. The maximum value of J which could thus be obtained for what we called "low- N " solutions is on the order of 380-400. This was dubbed the "error barrier" because the only way to break past these values for J would be to reduce the error terms, which in turn is predicated on settling much more than just a handful of stars. The error barrier was broken about a day after the first low- N solutions were being returned. Plots of the top fourteen solutions are shown in Figs. 5 and 6; the Sun is in green, stars settled by Fast Ships are in magenta, by Settlement Pods in blue, and by Settler Ships in orange.

Table 3. Final results of the top 25 teams

Rank	Team Name	N	ΔV_{used} (km/s)	ΔV_{max} (km/s)	J
1	NUDT&XSCC	3798	0.812701E+06	0.152170E+07	3101.14604
2	Tsinghua LAD - XINGYI	2806	0.624757E+06	0.112500E+07	2070.53723
3	ESA-ACT	2652	0.660946E+06	0.106350E+07	1996.11072
4	The Aerospace Corp.	2435	0.769120E+06	0.976800E+06	1559.28104
5	HIT_BACC	2855	0.714294E+06	0.114520E+07	1167.423
6	CSU	1246	0.181974E+06	0.501200E+06	1111.00887
7	Sapienza-PoliTo	1013	0.271417E+06	0.408200E+06	946.450958
8	worhp2orb	3235	0.107048E+07	0.129620E+07	873.309569
9	1-2-B-#1	1863	0.403540E+06	0.748100E+06	802.932024
10	Team Kataskopoi	1352	0.426588E+06	0.543800E+06	597.045676
11	NASA GRC	1021	0.232315E+06	0.411500E+06	544.445771
12	Team Jena	5	0.617327E+02	0.540000E+04	368.847689
13	NASA LaRC	754	0.231610E+06	0.303500E+06	360.787798
14	NUDT-G301	1347	0.413174E+06	0.541500E+06	360.736571
15	NASA MSFC	2	0.239954E+02	0.300000E+04	330.407412
16	UMich	3	0.441739E+02	0.380000E+04	321.192929
17	CU Boulder	5	0.778346E+02	0.540000E+04	307.313235
18	TM	494	0.630813E+05	0.200400E+06	297.958738
19	NUAA-ASTL	5	0.767176E+02	0.540000E+04	277.570699
20	IRSIBJ	5	0.642709E+02	0.540000E+04	268.040151
21	KAIST	2	0.226858E+02	0.300000E+04	242.605091
22	Team BIT	758	0.230746E+06	0.306600E+06	237.9109
23	Team Rocket	1	0.937812E+01	0.150000E+04	207.829574
24	Toso & Herrera	5	0.630259E+02	0.540000E+04	203.648553
25	MSU-RAS-RUDN	968	0.180743E+06	0.390000E+06	201.583171

The largest number of Settlement Pods dropped off by a single Mother Ship was 6; a number of teams submitted such solutions, including several in the top 14, one of which, the NASA LaRC solution, had all three Mother Ships dropping off 6 Pods.

Amongst the top 25 teams, all 9 that had low- N solutions settled star 51919, either with a Settlement Pod or a Fast Ship. Seven of those nine settled star 96507, and 5 settled 87651. None of the leaderboard solutions that broke the error barrier settled any of those three stars.

All teams that broke the error barrier settled 1021 or more stars. The significance of this number is that it is the minimum number of stars that would be needed to drive E_r to zero even under the assumption that the radius for each star could be freely specified (not drawn from the given set of stars). The E_θ term can be made very small with much fewer stars. Interestingly, the final leaderboard had a solution with 1021 stars.

CONCLUSION

The tenth Global Trajectory Optimisation Competition, GTOC X, saw wide participation from teams around the world, just edging out the level of participation seen in GTOC9, and almost twice the participation of previous GTOCs. The breaking of the error barrier was a complex endeavor, and was accomplished by eleven teams. The merit function and constraints made this a multi-faceted problem, which gave teams many avenues to explore. The spatial distribution objective was perhaps the most foreign and most difficult to tackle. We trust that the methods developed for optimizing the spatial distribution will bear fruit in related areas of traditional mission design. We also hope that this unconventional problem was a good vehicle to look at the methods of trajectory optimization

anew, to inspire young mission designers, and to foster collaborations between mission designers and the broader optimization community. The winners of GTOC X, the joint NUDT & XSCC team, have graciously taken on the mantle of hosting the next GTOC, tentatively planned for 2021.

ACKNOWLEDGMENT

The authors thank the participating teams for their enthusiastic and varied approaches to solving the GTOC X problem. This research was performed in part at the Jet Propulsion Laboratory, California Institute of Technology under a contract with the National Aeronautics and Space Administration.

REFERENCES

- [1] The Global Trajectory Optimisation Portal: The America’s cup of rocket science, https://sophia.estec.esa.int/gtoc_portal/, accessed Aug. 2019.
- [2] J. Binney and S. Tremaine, *Galactic Dynamics*, 2nd ed., 2008, Princeton Univ. Press, Princeton, NJ.
- [3] Gaia Collaboration, D. Katz, T. Antoja, M. Romero-Gómez, R. Drimmel, *et al.*, “Gaia Data Release 2: Mapping the Milky Way disc kinematics,” *Astronomy & Astrophysics*, manuscript no. Gaia-DR2-MWmap, April 26, 2018.
- [4] Dorota M. Skowron, Jan Skowron, Przemek Mróz, Andrzej Udalski, *et al.*, “A three-dimensional map of the Milky Way using classical Cepheid variable stars,” *Science*, 365, 478-482, 2 August 2019.
- [5] Pijushpani Bhattacharjee, Soumini Chaudhury, and Susmita Kundu, “Rotation Curve of the Milky Way out to ~ 200 kpc,” *The Astrophysical Journal*, 785:63 (13pp), 2014 April 10.
- [6] Gaia Collaboration, T. Prusti, J. H. J. de Bruijne, A. G. A. Brown, A. Vallenari, C. Babusiaux, C. A. L. Bailer-Jones, U. Bastian, M. Biermann, D. W. Evans, *et al.*, “The Gaia mission,” *Astronomy and Astrophysics*, vol. 595, p. A1, Nov 2016.
- [7] Gaia Collaboration, A. G. A. Brown, A. Vallenari, T. Prusti, J. H. J. de Bruijne, C. Babusiaux, C. A. L. Bailer-Jones, M. Biermann, D. W. Evans, L. Eyer, *et al.*, “Gaia Data Release 2. Summary of the contents and survey properties,” *Astronomy and Astrophysics*, vol. 616, p. A1, Aug. 2018.
- [8] X. Luri, A. G. A. Brown, L. M. Sarro, F. Arenou, C. A. L. Bailer-Jones, A. Castro-Ginard, J. de Bruijne, T. Prusti, C. Babusiaux, and H. E. Delgado, “Gaia Data Release 2. Using Gaia parallaxes,” *Astronomy and Astrophysics*, vol. 616, p. A9, Aug. 2018.
- [9] L. L. Watkins, R. P. van der Marel, S. T. Sohn, and N. W. Evans, “Evidence for an intermediate-mass milky way from gaia dr2 halo globular cluster motions,” *The Astrophysical Journal*, vol. 873, no. 2, p. 118, 2019.
- [10] J. Barnes and P. Hut, “A hierarchical $\mathcal{O}(N \log N)$ force-calculation algorithm,” *Nature*, vol. 324, no. 6096, p. 446, 1986.
- [11] M. Zitelli, “N-body_barnes_hut.” https://github.com/MateusZitelli/N-Body_Barnes_Hut, 2012.
- [12] GTOC X competition website, <https://gtocx.jpl.nasa.gov>, April-August 2019.

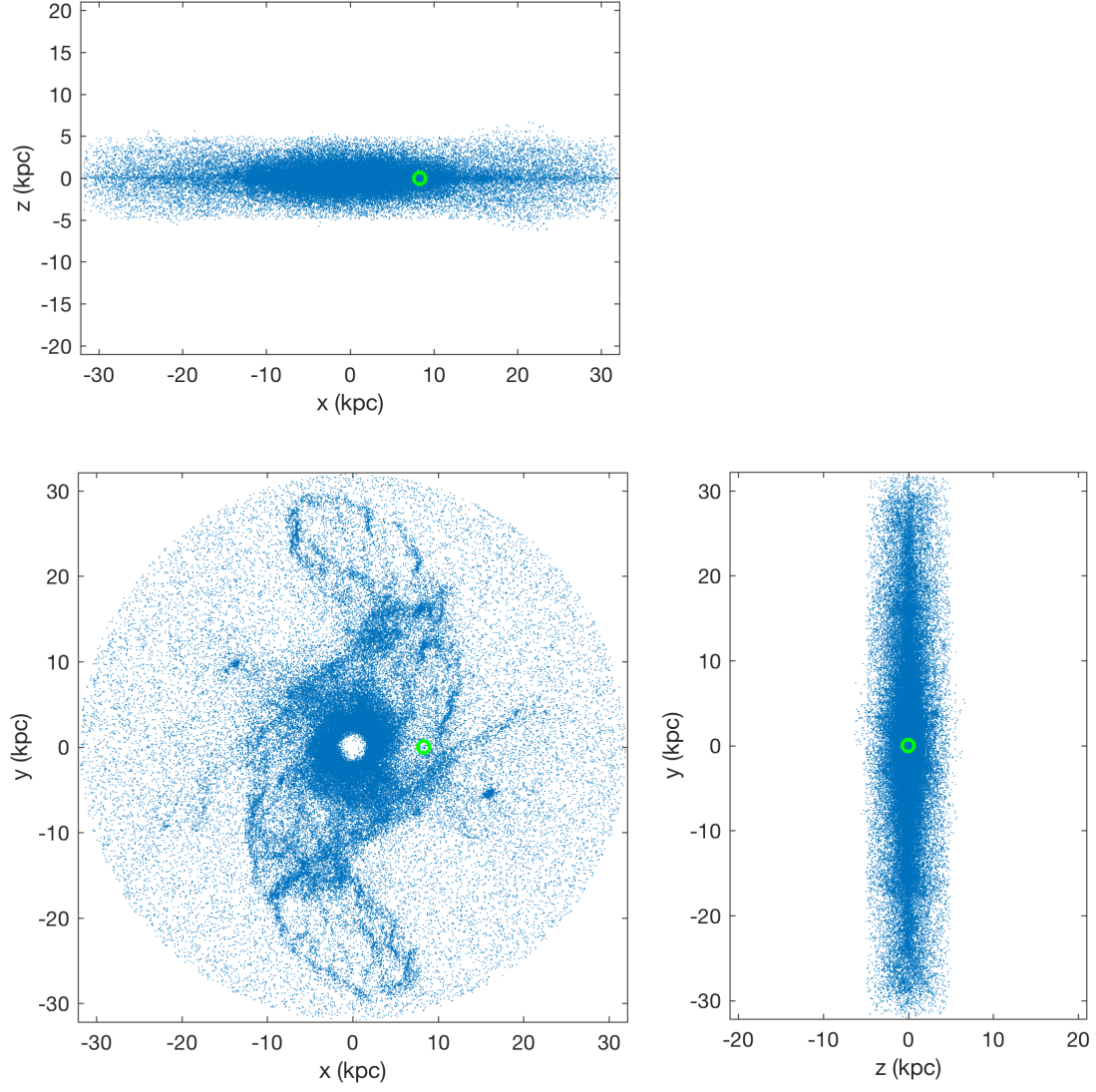


Figure 3. Distribution of stars in the galaxy at $t = 0$. Sun is in green.

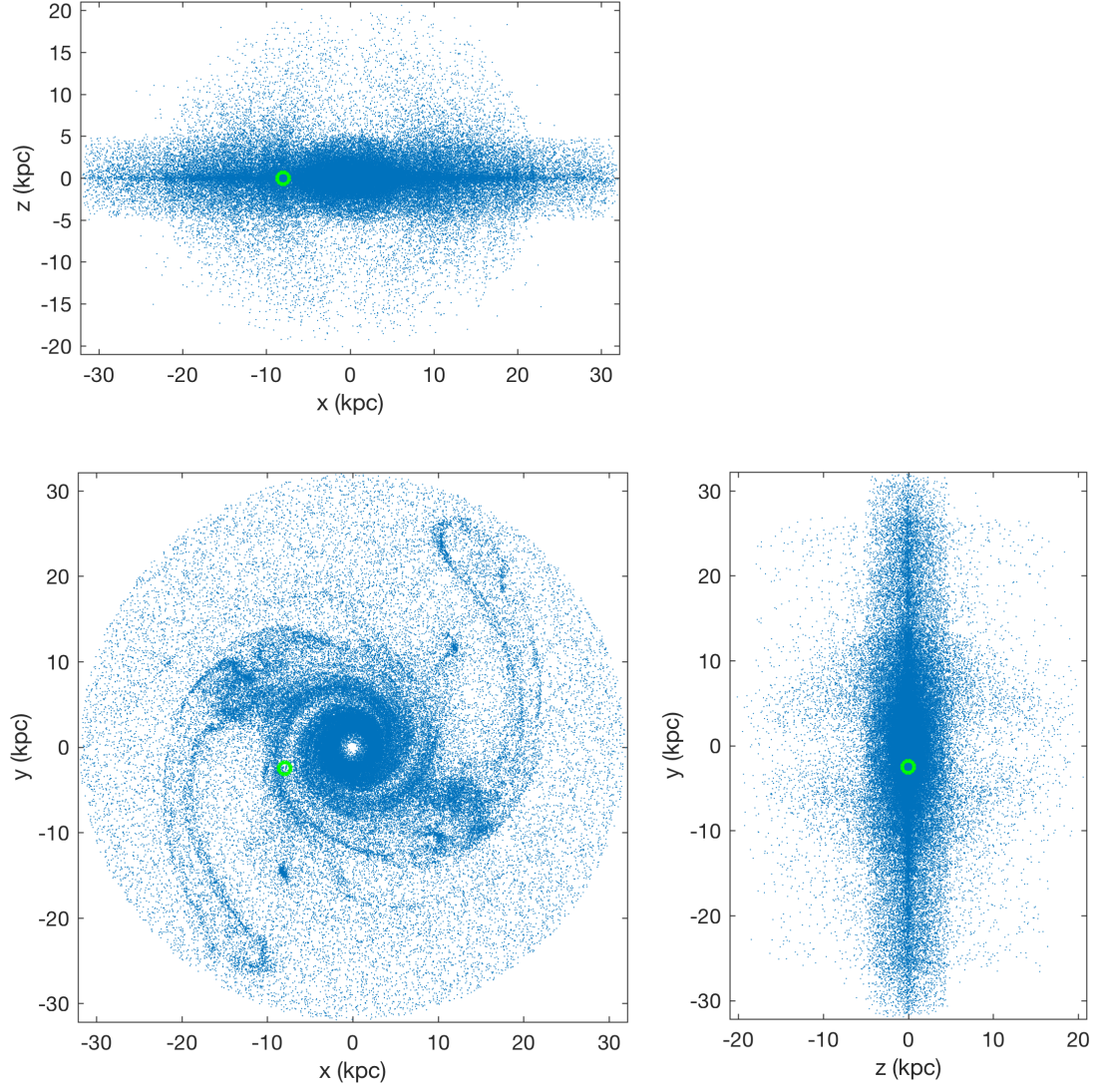
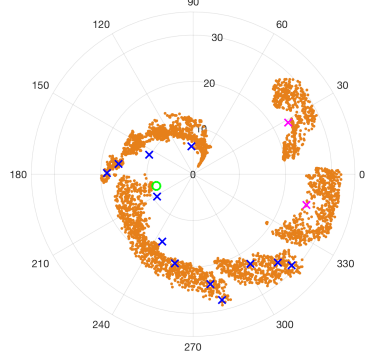
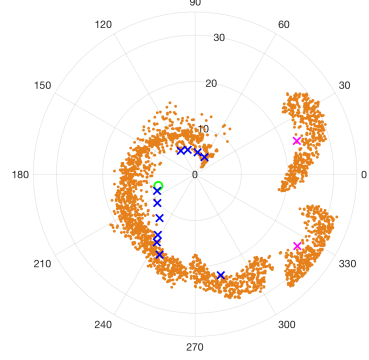


Figure 4. Distribution of stars in the galaxy at $t = 90$ Myr. Sun is in green.

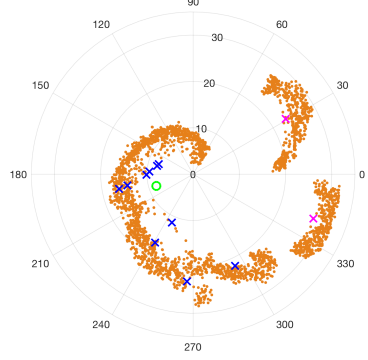
submission_69_2019_06_13_03_55_40 - NUDT&XSCC
N JnoB Nerr Etheta Er Etot DVused max/usd
3798 3101.1 1656.2 2.3 1.1 3.4 812701 1.87



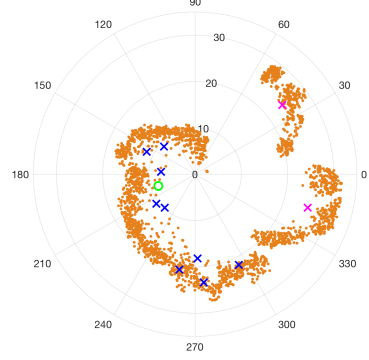
submission_241_2019_06_12_09_19_45 - Tsinghua LAD - XINGYI
N JnoB Nerr Etheta Er Etot DVused max/usd
2806 2070.5 1149.9 1.9 3.3 5.1 624757 1.80



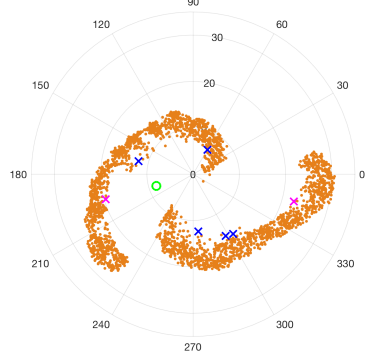
submission_116_2019_06_12_21_45_07 - ESA
N JnoB Nerr Etheta Er Etot DVused max/usd
2652 1996.1 1240.5 2.1 2.1 4.3 660946 1.61



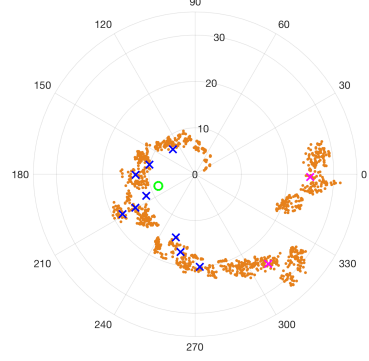
submission_222_2019_06_12_15_35_39 - Aerospace
N JnoB Nerr Etheta Er Etot DVused max/usd
2435 1559.3 1227.8 2.6 1.4 4.0 769120 1.27



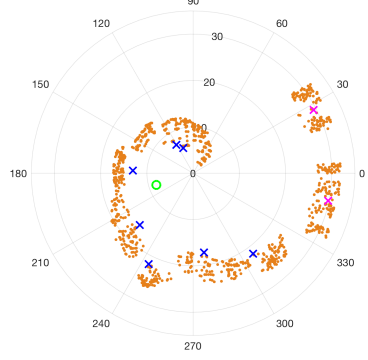
submission_247_2019_06_13_03_45_20
N JnoB Nerr Etheta Er Etot DVused max/usd
2855 1167.4 728.2 7.0 3.2 10.2 714294 1.60



submission_229_2019_06_12_14_57_40 - CSU
N JnoB Nerr Etheta Er Etot DVused max/usd
1246 1111.0 403.4 8.3 8.5 16.8 181974 2.75



submission_185_2019_06_12_21_49_46 - PoliTo
N JnoB Nerr Etheta Er Etot DVused max/usd
1013 946.5 629.3 1.9 4.1 6.0 271417 1.50



submission_213_2019_06_12_17_19_53 - worhp2orb
N JnoB Nerr Etheta Er Etot DVused max/usd
3235 873.3 721.2 5.6 5.2 10.8 1.07048e+06 1.21

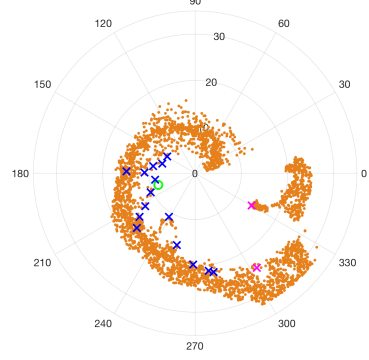
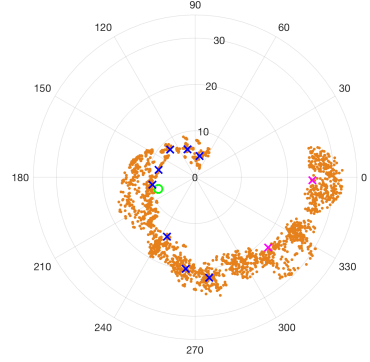
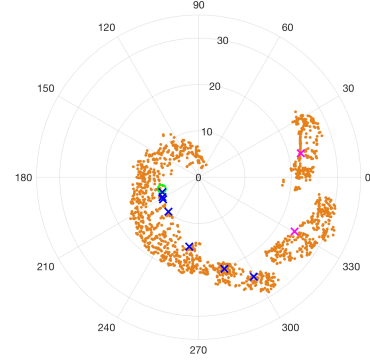


Figure 5. Top 8 solutions: Positions of settled stars at $t=90$ Myr.

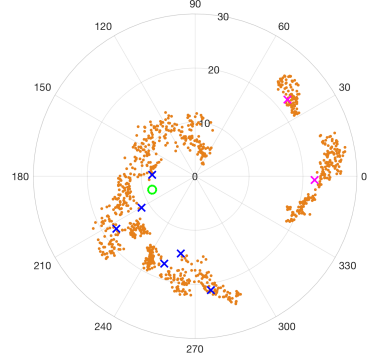
submission_153_2019_06_12_21_48_01 - 1-2-B-#1
N JnoB Nerr Etheta Er Etot DVused max/usd
1863 802.9 433.1 5.5 12.2 17.7 403540 1.85



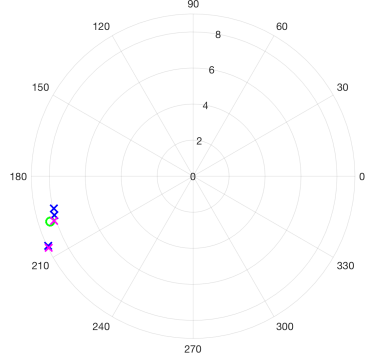
submission_192_2019_06_12_10_22_20 - Kataskopoi
N JnoB Nerr Etheta Er Etot DVused max/usd
1352 597.0 468.4 4.9 9.1 14.0 426588 1.27



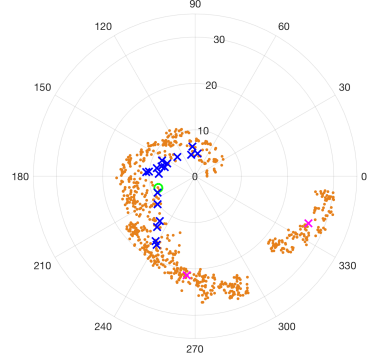
submission_282_2019_06_12_15_59_55 - NASA GRC
N JnoB Nerr Etheta Er Etot DVused max/usd
1021 544.4 307.4 12.8 9.9 22.7 232315 1.77



submission_84_2019_05_23_06_45_02 - Jena
N JnoB Nerr Etheta Er Etot DVused max/usd
5 207.9 2.4 1820.5 386.7 2207.2 61.7327 87.47



submission_81_2019_06_12_14_35_38 - NASA LaRC
N JnoB Nerr Etheta Er Etot DVused max/usd
754 360.8 275.3 9.6 13.5 23.1 231610 1.31



submission_144_2019_06_03_20_19_37 - NUDT-G301
N JnoB Nerr Etheta Er Etot DVused max/usd
1347 349.5 266.7 6.2 23.9 30.1 413174 1.31

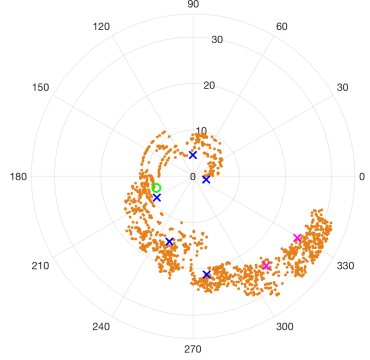


Figure 6. Rank 9-14 solutions: Positions of settled stars at $t=90$ Myr.